

Nonlinear electrodynamics in layered superconductors

V. A. Yampol'skii,^{1,2} Sergey Savel'ev,^{1,3} A. L. Rakhmanov,^{1,3,4} and Franco Nori^{1,5}

¹*Advanced Science Institute, The Institute of Physical and Chemical Research (RIKEN), Wako-shi, Saitama, 351-0198, Japan*

²*A. Ya. Usikov Institute for Radiophysics and Electronics, Ukrainian Academy of Sciences, 61085 Kharkov, Ukraine*

³*Department of Physics, Loughborough University, Loughborough LE11 3TU, United Kingdom*

⁴*Institute for Theoretical and Applied Electrodynamics, Russian Academy of Sciences, 125412 Moscow, Russia*

⁵*Department of Physics, Center for Theoretical Physics, Applied Physics Program, Center for the Study of Complex Systems, The University of Michigan, Ann Arbor, Michigan 48109-1040, USA*

(Received 5 December 2007; revised manuscript received 29 May 2008; published 15 July 2008)

We analyze theoretically the effect of a weak nonlinearity on the propagation of Josephson plasma waves in layered superconductors. The nonlinearity originates from the Josephson relation between the current density across superconducting layers and gauge-invariant phase difference of the order parameter. We show that strong nonlinear effects can be observed for electromagnetic waves with frequency slightly above or slightly below the plasma frequency. We study the nonlinear plasma resonance accompanied by the hysteretic dependence of the wave amplitude on the frequency. This hysteresis transforms the continuous terahertz radiation into a series of short electromagnetic high-amplitude pulses. We also consider the propagation of a nonlinear terahertz beam localized in the direction across the superconducting layers. This phenomenon is an analog of the self-focusing effect in nonlinear optics. The nonlinear phenomena in layered superconductors considered here can be potentially useful for the design of a new generation of terahertz devices.

DOI: [10.1103/PhysRevB.78.024511](https://doi.org/10.1103/PhysRevB.78.024511)

PACS number(s): 74.50.+r, 74.78.Fk

I. INTRODUCTION

The physical properties of layered superconductors, e.g., $\text{Bi}_2\text{Sr}_2\text{CaCu}_2\text{O}_{8+\delta}$, have attracted considerable interest from many research groups. The strongly anisotropic high temperature $\text{Bi}_2\text{Sr}_2\text{CaCu}_2\text{O}_{8+\delta}$ superconductors are characteristic members of this family. Intensive experimental studies of the c -axis conductivity in layered high temperature superconductors (HTSC) justify a model in which the superconducting CuO_2 layers are coupled by intrinsic Josephson junctions.¹ The Josephson current flowing along the c axis interacts with the electromagnetic field inside the insulating dielectric layers, producing Josephson plasma waves (JPWs).¹⁻¹² In other words, the layered structure of superconductors favors the propagation of electromagnetic waves. A challenge is to excite¹³ and to control^{14,15} electromagnetic waves in $\text{Bi}_2\text{Sr}_2\text{CaCu}_2\text{O}_{8+\delta}$ (BSCCO) samples because of their subterahertz and terahertz frequency range,^{11,16} which is still hardly reachable for both electronic and optical devices.

Linear electromagnetic phenomena, including Josephson plasma resonance, propagation of Josephson plasma waves, reflectivity, and transmissivity, etc, in anisotropic superconductors were considered in many experimental and theoretical works (see, e.g., Refs. 17–28). Here, we consider essentially *nonlinear* phenomena in JPWs propagation, originated from the nonlinear Josephson relation between the current density J across the layers and gauge-invariant phase difference φ , i.e., $J = J_c \sin \varphi$. Here, J_c is the maximum Josephson current density.

The electrodynamics of layered superconductors is described by a set of coupled sine-Gordon equations for the gauge-invariant interlayer phase difference φ (see Refs. 29–34). In the strongly nonlinear regime ($\varphi \sim \pi$), the sine-Gordon equation possesses soliton and breather solutions.^{35,36} However, the nonlinearity becomes crucial

even at small wave amplitudes, at $|\varphi| \ll 1$, due to a gap in the spectrum of the JPWs. In Refs. 38 and 39, we discussed such phenomena. Some of these, (e.g., JPWs self-focusing effects, the pumping of weaker waves by a stronger one, nonlinear plasma resonances, and nonlinear surface and wave-guide propagation) have analogs³⁷ in traditional nonlinear optics. In addition, the unusual stop-light phenomenon caused by both nonlinearity and dissipation was predicted in Ref. 38.

In this paper, we consider in detail two important nonlinear phenomena that can be observed just above or slightly below the Josephson plasma frequency ω_J . One of them is the nonlinear geometric Josephson plasma resonance that can be observed in layered superconductors when $\omega > \omega_J$. This effect, being well-known in nonlinear physics, was not investigated for Josephson media until recently, despite the fact that the one-dimensional sine-Gordon equation was previously studied by many research groups (see, e.g., Ref. 35 and references therein).

Another phenomenon considered here is specific for layered Josephson media for frequencies ω below ω_J . We have predicted in Ref. 38, and study here, the propagation of a nonlinear terahertz beam localized across the layers, which is an analog of the self-focusing effect in nonlinear optics.

II. COUPLED SINE-GORDON EQUATIONS

Consider a layered superconductor with the layers in the xz plane and the y axis along the c axis. We assume that the magnetic field H is along the z direction and study the waves propagating along the layers in the x direction. In this case, the electric field \mathbf{E} of the JPWs has only x and y components, E_x , E_y , and the fields do not depend on z . The electromagnetic field inside the superconductor is defined by the distribution of the gauge-invariant phase difference $\varphi_l(x, t)$ of the order parameter between l th and $(l+1)$ th layers. The dynam-

ics of $\varphi_l(x,t)$ can be described by a set of coupled sine-Gordon equations. These equations can be derived either in the model of S-I (superconductor-insulator) multilayered system²⁹ or on the basis of the Lawrence-Doniach model.^{30–32} The latter approach is more natural for HTSC and we will use it below. In this case, the equations related to $\varphi_l(x,t)$ and the magnetic field H_l between the l th and $(l+1)$ th layers can be written as^{40,41}

$$\frac{\partial^2 \varphi_l}{\partial t^2} = (\alpha \partial_l^2 - 1) \left(\nu_c \frac{\partial \varphi_l}{\partial t} + \sin \varphi_l - \frac{\partial \tilde{h}_l}{\partial x} \right), \quad (1)$$

$$\left[\partial_l^2 - \frac{D^2}{\lambda_{ab}^2} \left(1 + \nu_{ab} \frac{\partial}{\partial t} \right) \right] \tilde{h}_l + \frac{D^2}{\lambda_{ab}^2} \left(1 + \nu_{ab} \frac{\partial}{\partial t} \right) \frac{\partial \varphi_l}{\partial x} = 0, \quad (2)$$

where the dimensionless coordinates, time, and magnetic field are introduced according to

$$x \rightarrow \frac{x}{\lambda_c}, \quad t \rightarrow \omega_J t, \quad \tilde{h}_l = \frac{H_l}{H_0}. \quad (3)$$

Here, λ_{ab} and $\lambda_c = c/(\omega_J \epsilon^{1/2})$ are the London penetration depths across and along the layers, respectively, the operator ∂_l^2 is defined as $\partial_l^2 f_l = f_{l+1} + f_{l-1} - 2f_l$, α is the parameter of the capacitive coupling,

$$\omega_J = (8\pi e D J_c / \hbar \epsilon)^{1/2}$$

is the Josephson plasma frequency. The characteristic field H_0 is

$$H_0 = \frac{\Phi_0}{2\pi D \lambda_c}. \quad (4)$$

Moreover, J_c is the maximum Josephson current, ϵ is the interlayer dielectric constant, D is the interlayer spacing, and Φ_0 is the flux quantum. The dissipation parameters,

$$\nu_{ab} = 4\pi \sigma_{ab} / \epsilon \gamma^2 \omega_J, \quad \nu_c = 4\pi \sigma_c / \epsilon \omega_J, \quad (5)$$

are determined by the quasiparticle conductivities, σ_{ab} and σ_c , along and perpendicular to the layers, respectively, $\gamma = \lambda_c / \lambda_{ab}$ is the anisotropy parameter. Note that $\nu_c \ll \nu_{ab} \ll 1$ for BSCCO.⁴¹ We normalize the y coordinate to λ_{ab} , $y \rightarrow y/\lambda_{ab}$ and denote the position of the l th layer as y_l . When deriving Eqs. (1) and (2), the quasiparticle charge imbalance and displacement current in the ab plane are neglected. The spatial variations in the y direction of fields inside the very thin superconducting layers and the magnetic-field dependence of σ_{ab} and σ_c are also ignored.

In the present work, we study weakly nonlinear plasma waves with frequencies near the plasma resonance ($\omega \sim 1$) varying on a large scale, Δy , in the y direction compared with the interlayer spacing D . These allow us to simplify Eqs. (1) and (2). We can present a solution φ_l as a Fourier series

$$\varphi_l = \sum_q \varphi_{ql}(x,t) \exp(iqy_l),$$

then

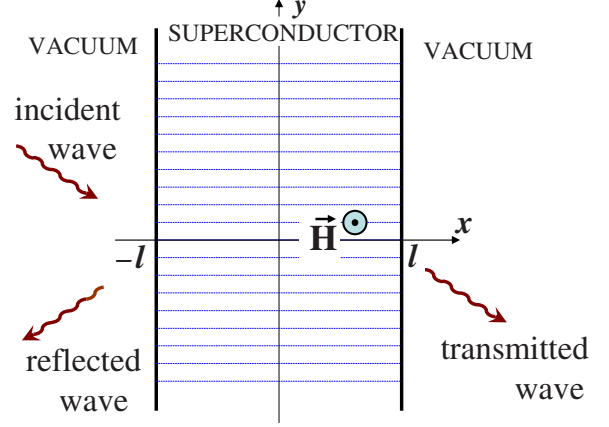


FIG. 1. (Color online) Geometry of the problem. A terahertz wave irradiates a slab of layered superconductor that occupies the region $-l < x < l$. The superconducting layers are parallel to the xz plane.

$$\partial_l^2 \varphi_l = \sum_q \tilde{q}^2 \varphi_{ql}(x,t) \exp(iqy_l),$$

where $\tilde{q}^2 = 2(1 - \cos qD/\lambda_{ab})$. The condition $\Delta y \gg D$ means that only the terms φ_{ql} with $qD/\lambda_{ab} \ll 1$ are of importance. Thus, we can approximate $\tilde{q}^2 = (qD/\lambda_{ab})^2$ and use Eqs. (1) and (2) in the continuum limit substituting $\partial_l^2 \rightarrow (D/\lambda_{ab})^2 \partial^2 / \partial y^2$. Moreover, we can neglect the term with the capacitive coupling $\alpha \partial_l^2$ in Eq. (1) since $\alpha < 1$ in HTSC.^{41,42} As a result, we derive from Eqs. (1) and (2)

$$\left(1 + \nu_{ab} \frac{\partial}{\partial t} - \frac{\partial^2}{\partial y^2} \right) \left(\frac{\partial^2 \varphi}{\partial t^2} + \nu_c \frac{\partial \varphi}{\partial t} + \sin \varphi \right) = \left(1 + \nu_{ab} \frac{\partial}{\partial t} \right) \frac{\partial^2 \varphi}{\partial x^2}. \quad (6)$$

The dissipation parameters are small in HTSC, $\nu_{ab}, \nu_c \ll 1$. So, we omit terms with ν_{ab} and ν_c . The applicability of this simplification is discussed at the ends of Secs. III and IV.

We investigate the effects of a weak nonlinearity and expand $\sin \varphi$ in Eq. (6) up to third power in φ . Thus, we arrive at our basic equation for further study,

$$\left(1 - \frac{\partial^2}{\partial y^2} \right) \left(\frac{\partial^2 \varphi}{\partial t^2} + \varphi - \frac{\varphi^3}{6} \right) - \frac{\partial^2 \varphi}{\partial x^2} = 0, \quad (7)$$

Below, we analyze Eq. (7) with its corresponding boundary conditions by means of an asymptotic expansion taking into account that the wave frequency ω is close to ω_J , that is, $|1 - \omega^2| \ll 1$ in dimensionless units.

III. NONLINEAR PLASMA RESONANCE

Consider an electromagnetic wave with frequency $\omega > 1$ and wave vector $\mathbf{k} = (k_0, q)$, incident from the vacuum, $x < -l$, at the edge of a slab of a layered superconductor, $-l < x < l$, Fig. 1. The magnetic field \mathbf{H} of the wave has only the z component while the electric field \mathbf{E} contains both x and y components. In dimensionless units for the wave in vacuum at $x < -l$, we have

$$H = H_i \exp(ik_0 x) + H_r \exp(-ik_0 x), \quad (8)$$

$$E_x = -\frac{q\sqrt{\epsilon}}{\gamma\omega}H, \quad (9)$$

$$E_y = \frac{k_0\sqrt{\epsilon}}{\omega}[H_i \exp(ik_0x) - H_r \exp(-ik_0x)], \quad (10)$$

where H_i and H_r are the amplitudes of the incident and reflected waves. Here and below we omit the multiplier $\exp(-i\omega t + iqy)$. The dispersion law for the wave in the vacuum has the form

$$\frac{q^2}{\gamma^2} + k_0^2 = \frac{\omega^2}{\epsilon}.$$

In the half-space $x > l$, there exists only a transmitted wave with

$$H = H_t \exp(ik_0x), \quad E_x = -\frac{q\sqrt{\epsilon}}{\gamma\omega}H, \quad (11)$$

$$E_y = \frac{k_0\sqrt{\epsilon}}{\omega}H_t \exp(ik_0x). \quad (12)$$

The relation between the gauge-invariant phase difference and the y component of the electric field in the superconducting sample can be presented as³²

$$E_y = \frac{H_0}{\sqrt{\epsilon}} \frac{\partial \varphi}{\partial t}. \quad (13)$$

The nonlinear relation between the phase difference φ and the magnetic field H can be derived from the Maxwell equation

$$\text{curl } \mathbf{H} = \frac{4\pi}{c} \mathbf{J} + \frac{\epsilon}{c} \frac{\partial \mathbf{E}}{\partial t}. \quad (14)$$

Using the expression

$$J_y = J_c \sin \varphi \approx J_c \cdot \left(\varphi - \frac{\varphi^3}{6} \right) \quad (15)$$

for the y component of the current density \mathbf{J} we obtain

$$-\frac{1}{\sqrt{\epsilon}} \frac{\partial H}{\partial x} = \frac{H_0}{\epsilon} \left(\varphi - \frac{\varphi^3}{6} \right) + \frac{\partial E_y}{\partial t}. \quad (16)$$

A. Linear approximation

Equation (7) can be solved by a standard perturbative approach. First, we examine this problem in the linear approximation and seek a solution for JPWs in the sample in the form of a sum of waves propagating forward and backward,

$$H = A \exp(ikx) + B \exp(-ikx), \quad (17)$$

$$\varphi = a \exp(ikx) + b \exp(-ikx), \quad (18)$$

with the dispersion law

$$k^2 = (\omega^2 - 1)(q^2 + 1). \quad (19)$$

From Eqs. (13), (4), and (16)–(18) we find:

$$\frac{\partial H}{\partial x} = H_0(\omega^2 - 1)\varphi, \quad (20)$$

the relations between the amplitudes A, B and a, b ,

$$a = \frac{ikA}{H_0(\omega^2 - 1)}, \quad b = -\frac{ikB}{H_0(\omega^2 - 1)}, \quad (21)$$

and the expression for the electric field E_y ,

$$E_y = \frac{k\omega}{\sqrt{\epsilon}(\omega^2 - 1)}[A \exp(ikx) - B \exp(-ikx)]. \quad (22)$$

Equation (14) relates also E_x and H at the sample edges,

$$E_x = -\frac{q}{\gamma\omega\sqrt{\epsilon}}H, \quad x = \pm l, \quad (23)$$

since $J_x = 0$ at these surfaces.

Now we should match the solutions in vacuum and in the sample requiring the continuity of the magnetic field and the tangential component of the electric field, E_y , at the sample boundaries. This yields

$$H_i \exp(-ik_0l) + H_r \exp(ik_0l) = A \exp(-ikl) + B \exp(ikl),$$

$$H_i \exp(-ik_0l) - H_r \exp(ik_0l) = Q(\omega)[A \exp(-ikl) - B \exp(ikl)],$$

$$H_t \exp(ik_0l) = A \exp(ikl) + B \exp(-ikl),$$

$$H_t \exp(ik_0l) = Q(\omega)[A \exp(ikl) - B \exp(-ikl)]a, \quad (24)$$

where

$$Q(\omega) = \frac{k\omega^2}{k_0\epsilon(\omega^2 - 1)}.$$

Solving these algebraic equations, we express all the amplitudes (A, B, H_r, H_t) via the amplitude H_i of the incident wave,

$$A = \frac{2(1+Q)H_i \exp(-i(k_0+k)l)}{(1+Q)^2 \exp(-2ikl) - (1-Q)^2 \exp(2ikl)}, \quad (25)$$

$$B = -\frac{2(1-Q)H_i \exp(-i(k_0-k)l)}{(1+Q)^2 \exp(-2ikl) - (1-Q)^2 \exp(2ikl)}, \quad (26)$$

$$H_r = -i(1-Q)\sin(2kl)A \exp(-i(k_0-k)l), \quad (27)$$

$$H_t = \frac{2Q}{1+Q}A \exp(-i(k_0-k)l). \quad (28)$$

One can see that the reflected wave disappears and the amplitudes of the JPW in the sample increase under the resonance condition $kl = \pi n/2$, where n is an integer. For this case, we derive from Eqs. (25)–(28)

$$A = i^n \frac{1+Q}{2Q} H_i \exp(-ik_0l), \quad (29)$$

$$B = (-i)^{n+1} \frac{1-Q}{2Q} H_i \exp(-ik_0 l), \quad (30)$$

$H_r=0$, and $|H_t|=|H_i|$. The values of Q_n for the resonance conditions are

$$Q_n \approx \frac{2\omega l(1+q^2)}{\sqrt{\epsilon\pi n}}. \quad (31)$$

Here, we take into account that $k_0 \approx \omega/\epsilon^{1/2}$ since $\gamma \gg 1$ for any layered high- T_c superconductor. If $Q_n \gg 1$, the resonance amplitudes of the wave in the sample, Eqs. (29) and (30), are much higher than far from the resonance. Thus, the electromagnetic energy stored in a sample of length $2L=2l\lambda_c$ increases, under resonance conditions, by a factor of about

$$Q_n^2 \sim 4L^2/\pi^2 \epsilon \lambda_c^2 n^2$$

in dimensional units. For a sample with $L=1$ cm, $\lambda_c=10^{-2}$ cm, and $\epsilon=20$, this value is about 200 for $n=1$.

B. Nonlinear effects

Now we take into account the nonlinearity in Eqs. (7) and (16), which gives rise to corrections to the wave amplitudes and the dispersion law (19). The main idea of the following calculations is analogous to that in the case of nonlinear oscillators.⁴³ It is of interest to study the system behavior near the first ($n=1$) resonance at ω close to 1, when $Q_1 \equiv Q \gg 1$ and the power of the JPW in the sample is maximum.

The nonlinearity results in a shift of the dispersion law, which we describe by replacing $k \rightarrow k^0 + \delta k$, where δk is a function of the wave amplitude. So, we rewrite the denominator Δ in Eqs. (25) and (26) as

$$\begin{aligned} \Delta &= (1+Q)^2 \exp(-2ikl) - (1-Q)^2 \exp(2ikl) \\ &= -2i(1+Q^2) \sin(2kl) + 4Q \cos(2kl). \end{aligned}$$

In the vicinity of the first resonance, $2kl = \pi + 2\delta k l$ and $Q \gg 1$, we obtain in first approximation

$$\Delta = -4Q(1-iQ\delta k l).$$

Substituting the last expression in Eqs. (25) and (26), we obtain

$$A = -B = \frac{iH_i \exp(-ik_0 l)}{2(1-iQ\delta k l)}. \quad (32)$$

Correspondingly, by means of Eqs. (29), (30), and (32), we derive

$$a = b = -\frac{H_i Q \sqrt{\epsilon} \exp(-ik_0 l)}{H_0 2a(1-iQ\delta k l)}. \quad (33)$$

To analyze the nonlinear problem, it is more suitable to use real values. Then, the phase difference in the first-order approximation can be written as

$$\varphi^{(0)} = a_0 [\cos(\omega t - kx - qy - \eta) + \cos(\omega t + kx - qy - \eta)], \quad (34)$$

where

$$\begin{aligned} a_0 &= \frac{QH_i}{2H_0} \frac{\sqrt{\epsilon}}{\sqrt{1+Q^2\delta k^2 l^2}}, \\ \eta &= -k_0 l + \tan^{-1}(Q\delta k l) \end{aligned} \quad (35)$$

We seek a solution of Eq. (7) in the form $\varphi = \varphi^{(0)} + \varphi^{(1)}$. Substituting this into Eq. (7) we find, in first-order approximation in $\varphi^{(1)}$ and δk ,

$$[(1+q^2)(1-\omega^2) + k^{(0)2}] \varphi^{(1)} = \left(1 - \frac{\partial^2}{\partial y^2}\right) \frac{\varphi^{(0)3}}{6} - 2k^{(0)} \delta k \varphi^{(0)}. \quad (36)$$

Following Ref. 43, the value of δk should be chosen to eliminate the first harmonics [resonance terms containing $\cos(\omega t \pm kx - qy - \eta)$] in the right-hand side of Eq. (36). Substituting Eq. (34) into Eq. (36) we obtain

$$\delta k = \frac{3(1+q^2)}{16k^{(0)}} a_0^2. \quad (37)$$

As in the case of ordinary nonlinear oscillators,⁴³ the shift of the dispersion law is proportional to a_0^2 .

Let us now consider a wave frequency not equal to the resonance frequency and different from ω_{res} by a small slowly-varying value $\omega_{\text{det}}(t)$, i.e., $\omega(t) = \omega_{\text{res}} + \omega_{\text{det}}(t)$. In this case, the variation of the wave vector,

$$\delta k_\omega = \frac{\partial k}{\partial \omega} \omega_{\text{det}} = \omega_{\text{det}} \left(\frac{1+q^2}{\omega_{\text{res}}^2 - 1} \right)^{1/2}, \quad (38)$$

should be added to Eq. (37),

$$\delta k = \frac{2(1+q^2)l}{\pi} \left(\frac{3}{16} a_0^2 + \omega_{\text{det}} \right). \quad (39)$$

Here we take into account that $\omega_{\text{res}} \approx 1$ and $k^{(0)} = \pi/2l$. Substituting this relation into Eq. (35) we derive a self-consistency condition for the wave amplitude

$$f(a_0^2, \omega_{\text{det}}) = a_0^2 \left[1 + \alpha^2 \left(\frac{3a_0^2}{16} + \omega_{\text{det}} \right)^2 \right] - h^2 = 0, \quad (40)$$

where

$$h = \frac{(1+q^2)lH_i}{\pi H_0}, \quad \alpha = \frac{4(1+q^2)^2 l^3}{\pi^2 \sqrt{\epsilon}}. \quad (41)$$

Equation (40) defines the dependence of the wave amplitude a_0 , near the resonance, on the detuning frequency ω_{det} , and the amplitude H_i of the incident wave. The function $a_0(\omega_{\text{det}})$ is shown in Fig. 2 for different H_i . One can see that this dependence is single-valued if H_i is smaller than some critical value H_{cr} . When $H_i > H_{\text{cr}}$, there is an interval of frequencies where the function $a_0(\omega_{\text{det}})$ has three branches. As usual, the intermediate branch is unstable while the lower and upper branches are stable. These stable branches can be reached when $\omega_{\text{det}}(t)$ either increases or decreases. As a result, a hysteresis in the $a_0(\omega_{\text{det}})$ dependence can be observed if $H_i > H_{\text{cr}}$. Obviously, to observe the hysteresis jumps in $a_0(t)$, the magnitude of the frequency change should exceed a critical value, i.e., $\omega_{\text{det}} > |\omega_{\text{det}}^{\text{(cr)}}|$.

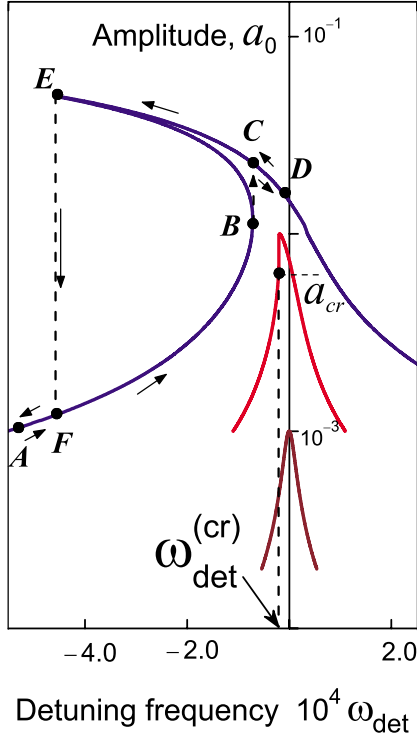


FIG. 2. (Color online) Amplitude a_0 (of the nonlinear Josephson plasma wave inside the sample) versus the detuning frequency ω_{det} near a resonance, for different incident wave amplitudes. The brown (lower) curve corresponds to $H_i/H_0=5 \cdot 10^{-5}$. The red (in the middle) curve is for the critical value $H_i/H_0=10^{-4}$. Note that, at stronger incident waves, the two stable and one unstable solutions for the amplitude of nonlinear waves inside the sample are possible. The blue (upper) curve is for $H_i/H_0=5 \cdot 10^{-4}$. The values of other parameters used here are: $l/\lambda_c=100$, $\epsilon=20$, $q=0.25$.

The critical values H_{cr} and $\omega_{\text{det}}^{(\text{cr})}$ can be derived from Eq. (40) and the condition $\partial^2 f / \partial a_0^2 = 0$. The latter condition results in

$$3\alpha^2 \left(\frac{3}{16}\right)^2 a_0^4 + \frac{3}{4} \alpha^2 \omega_{\text{det}}^2 a_0^2 + 1 + \alpha^2 \omega_{\text{det}}^2 = 0. \quad (42)$$

This is a quadratic equation with respect to a_0^2 . It has real roots if its discriminant $D(\omega_{\text{det}})$ is positive. Thus, the threshold frequency deviation $\omega_{\text{det}}^{(\text{cr})}$ is defined by the evident condition $D(\omega_{\text{det}}^{(\text{cr})})=0$. From this we obtain

$$\omega_{\text{det}}^{(\text{cr})} = -\frac{\sqrt{3}}{\alpha}. \quad (43)$$

From Eqs. (42) and (43) we calculate the critical amplitude a_{cr} that corresponds to $\omega_{\text{det}}^{(\text{cr})}$

$$a_{\text{cr}} = \frac{2^{5/2}}{3^{3/4} \alpha^{1/2}}. \quad (44)$$

Finally, by means of Eq. (40), we obtain the inequality to determine the minimum incident wave amplitude

$$h > h_{\text{cr}} = \frac{8\sqrt{2}|\omega_{\text{det}}^{(\text{cr})}|^{1/2}}{3}$$

necessary to observe the hysteresis effect. In dimensional units, this produces the condition

$$H_i > H_{\text{cr}} = \frac{2^{5/2} \pi}{3^{3/4}} \frac{\epsilon^{1/4}}{(1+q^2)^{5/2}} H_0. \quad (45)$$

Using the same values as for the estimate after Eq. (31), we obtain $\omega_{\text{det}}^{(\text{cr})} \approx -10^{-5}$. Thus, the critical detuning frequency is approximately -5 MHz for Josephson plasma frequency ~ 0.5 THz. The estimate for the critical amplitude gives the ratio $H_{\text{cr}}/H_0 \approx 10^{-4}$. If $D=1.5$ nm, then $H_0 \approx 21$ Oe and $H_{\text{cr}} \approx 2 \cdot 10^{-3}$ Oe.

The hysteresis of the wave amplitude can result in an interesting phenomenon: the transformation of the input continuous terahertz radiation into a set of short bursts with amplitudes significantly higher than the amplitude of the incident wave (see animation at <http://dml.riken.jp/nonlinear/nonlinear.swf>). Indeed, while the frequency of the incident wave increases approaching ω_{res} [corresponding to the $A \rightarrow B \rightarrow C \rightarrow D$ (or $ABCD$) route in Fig. 2], the energy of the electromagnetic wave is accumulated in the sample. When the frequency is decreased (route $DCEFA$ in Fig. 2), the amplitude of the wave decreases abruptly (sudden jump $E \rightarrow F$) and a significant part of the stored energy is released in the form of a short terahertz pulse.

Here, we neglect dissipation effects due to quasiparticle tunneling. These effects can suppress the nonlinear plasma resonance. To analyze the applicability of the obtained results, we study the dispersion law $k(\omega, q)$ taking into account terms in Eq. (6) with the dissipation parameters ν_{ab} and ν_c . Linearizing this equation under conditions the $\nu_{ab}, \nu_c, q^2 \ll 1$, we obtain

$$k^2 = (\omega^2 - 1 - i\nu_c \omega)(q^2 + 1 - iq^2 \nu_{ab} \omega). \quad (46)$$

Comparing this dispersion equation with the dispersion law Eq. (19), we conclude that the obtained results are valid if

$$q^2 \nu_{ab}, \nu_c < \omega_{\text{det}}. \quad (47)$$

C. Sample heating

The heating of the sample can also be important for the predicted nonlinear effects. Here, we derive the conditions under which the overheating ΔT is small and we can neglect the change in the sample properties. The heat power dissipated in the sample, per unit volume, is $\sigma_{ab} E_x^2 + \sigma_c E_y^2$. Following a standard approach used for estimating the superconductor overheating,⁴⁴ we can write ΔT as a sum of the temperature difference ΔT_1 , between the sample bulk and the sample surface, and ΔT_2 , between the sample surface and the ambient volume. The $\text{Bi}_2\text{Sr}_2\text{CaCu}_2\text{O}_{8+\delta}$ single crystals usually have the shape of a plate, with the smallest dimension $L_y \leq 0.1$ mm in the c direction. In this case, the ratio $\Delta T_2/\Delta T_1$ is determined by the Biot criterion,⁴⁴ that is, the ratio of the transverse thermal conductivity κ_c and the product of $L_y W$, where W is the surface heat transfer coefficient

also known as the Kapitza conductance. For HTSC single crystals in any realistic case $L_y W \ll \kappa_c$ and⁴⁴

$$\Delta T \approx \Delta T_2 = (\sigma_{ab} E_y^2 + \sigma_c E_y^2) L_y / W.$$

Using Eqs. (19), (22), and (23), we can rewrite the last condition for $(\omega-1) \approx \omega_{\text{det}}$ and $H_i = H_{\text{cr}}$ in the form

$$\Delta T \approx \frac{H_{\text{cr}}^2 \sigma_c L_y}{4W \epsilon \omega_{\text{det}}} \left(1 + \frac{q^2 \omega_{\text{det}} \sigma_{ab}}{\gamma^2 \sigma_c} \right). \quad (48)$$

Taking, for estimates, $\gamma = 500$, $\epsilon = 20$, $\sigma_c = 2 \cdot 10^{-3} \Omega^{-1} \text{cm}^{-1}$, $\sigma_{ab} = 4 \cdot 10^4 \Omega^{-1} \text{cm}^{-1}$,⁴¹ $W = 10^{-1} \text{W/cm}^2 \text{K}$ (cooling by liquid helium), or $10^3 \text{W/cm}^2 \text{K}$ (cooling by liquid nitrogen),⁴⁴ $H_{\text{cr}} = 2 \cdot 10^{-3} \text{Oe}$, $q = 1$, $\omega_{\text{det}} = 1 \cdot 10^{-4}$, and $L_y = 0.1 \text{mm}$, we obtain $\Delta T \approx 10^{-2} \text{K}$ (helium) and 10^{-6}K . Thus, we can neglect the sample heating in any case.

IV. LOCALIZED TERAHERTZ BEAM

Another example of a nonlinear effect in layered superconductors is the possible formation (below the plasma frequency ω_j) of plasma waves localized across the layers. The existence of such localized beams can be understood by means of a simple analysis of the coupled sine-Gordon equations [Eq. (7)] and the dispersion law [Eq. (19)] for the linear plasma waves. The tails of the localized beams can be considered as linear waves. They can propagate along the x direction with $\omega < \omega_j$ due to the concave profile of $\varphi(y)$. Indeed, Eq. (19) shows that the x component of the wave vector k can be real for the waves with $\omega < \omega_j$ only in the case of imaginary q , with $q^2 + 1 < 0$. In other words, the tails of the beam should have a form

$$\varphi \propto \exp(ikx - i\omega t \pm \kappa y)$$

with real κ . Note that such a concave profile of $\varphi(y)$ also describes surface Josephson plasma waves localized near the sample boundary.^{39,45,46} The middle part (the ‘‘peak’’) of the beam cannot have the concave profile of $\varphi(y)$. However, this part of the beam *can* propagate when $\omega < \omega_j$ due to the nonlinearity. Indeed, in the nonlinear regime, the cubic term φ^3 in Eq. (7) can change the sign of the sum in the second bracket if the wave amplitude exceeds some threshold value.³⁸ Thus, we can imagine the localized (in the y direction) beam consisting of two ‘‘linear tails’’ decaying as $\exp(-\kappa|y|)$, with $\kappa > 1$ when $|y| \rightarrow \infty$, that are connected with each other via the nonlinear ‘‘peak,’’ where the amplitude of the wave exceeds the threshold value.

We now seek a solution of Eq. (7) using the asymptotic expansion

$$\varphi = \sum_{n=0}^{\infty} a_{2n+1}(y) \sin[(2n+1)(\omega t - kx)]. \quad (49)$$

Here, we only keep the amplitudes a_{2n+1} of the odd harmonics because we study the cubic nonlinearity. For waves with amplitudes

$$a_1 \sim (1 - \omega^2)^{1/2} \ll 1,$$

the nonlinear term φ^3 in Eq. (7) is of the same order as the linear one, $\partial^2 \varphi / \partial t^2 + \varphi$, and even a weak nonlinearity plays a

key role in the wave propagation. Substituting the expansion (49) in the sine-Gordon Eq. (7), we obtain a set of ordinary equations for the harmonic amplitudes $a_{2n+1}(y)$. A standard analysis shows³⁸ that the amplitudes of higher harmonics decrease with increase of n as

$$a_{2n+1} \propto |1 - \omega^2|^{n+1/2}.$$

Therefore, we restrict our study to the first harmonics only. The equation for the amplitude of the first harmonics has the form,

$$\left(1 - \frac{d^2}{dy^2} \right) \left[(1 - \omega^2) a_1 - \frac{a_1^3}{8} \right] + k^2 a_1 = 0, \quad (50)$$

with boundary conditions

$$a_1(\pm \infty) = 0 \quad (51)$$

corresponding to a localized solution. Introducing the new variables,

$$A = \frac{a_1}{(1 - \omega^2)^{1/2}}, \quad \kappa = \frac{k}{(1 - \omega^2)^{1/2}}, \quad \xi = \kappa y, \quad (52)$$

we rewrite Eq. (50) in the form

$$\left[1 - \kappa^2 \frac{d^2}{d\xi^2} \right] \left(A - \frac{A^3}{8} \right) + \kappa^2 A = 0. \quad (53)$$

Using Eqs. (13) and (16), we obtain the relation between the phase amplitude $A(\xi)$ and the components of the electromagnetic field of the beam:

$$H = H(\xi) \cos(\omega t - kx), \quad (54)$$

$$H(\xi) = H_0 \frac{(1 - \omega^2)}{\kappa} h(\xi), \quad (55)$$

$$h(\xi) = -A(\xi) + \frac{A^3(\xi)}{8}, \quad (56)$$

$$E_x = E_x(\xi) \sin(\omega t - kx), \quad (57)$$

$$E_x(\xi) = -H_0 \frac{\lambda_{ab}}{\sqrt{\epsilon} \lambda_c} (1 - \omega^2) h'(\xi) \quad (58)$$

$$E_y = E_y(\xi) \cos(\omega t - kx), \quad (59)$$

$$E_y(\xi) = H_0 (1 - \omega^2)^{1/2} \frac{1}{\sqrt{\epsilon}} A(\xi). \quad (60)$$

Equation (50) has a first integral. After integration, we derive

$$\left(\frac{dA}{d\xi} \right)^2 = \frac{C + A^6 - 12A^4 \left(\kappa^2 + \frac{4}{3} \right) + 64A^2 (\kappa^2 + 1)}{\kappa^2 (8 - 3A^2)^2}. \quad (61)$$

Using this equation, we can construct the phase diagram in the (A, A') plane (here prime denotes the derivative with respect to ξ). For simplicity, we now restrict our analysis to the case when $\kappa \gg 1$, since this simplification does not

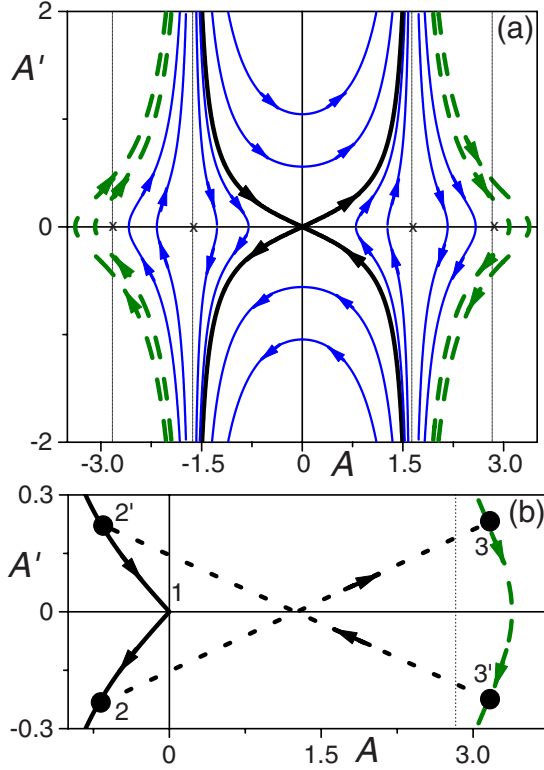


FIG. 3. (Color online) The phase diagram (A', A) of Eq. (62). (a) General appearance; (b) the parts of the phase trajectories that correspond to the localized beam (solid and dashed thick lines), dotted arrows represent φ -jumps. Vertical dotted lines correspond to $A = -\sqrt{8}, -\sqrt{8/3}, \sqrt{8/3}, \sqrt{8}$.

change the results qualitatively. In this limit, Eq. (61) yields

$$(A')^2 = -\frac{4}{3} + \frac{G}{(8 - 3A^2)^2}. \quad (62)$$

The phase diagram of Eq. (62), i.e., the set of $A'(A)$ curves for different constants G is shown in Fig. 3(a). According to the boundary conditions Eq. (51), the point $(0,0)$ in the phase diagram in Fig. 3 corresponds to $|y| = \infty$. Thus, the black solid lines at $|A(\xi)| < \sqrt{8/3}$ correspond to the tails of the beam. As it follows from Eq. (56), the value of A is negative at the tails if we demand the positiveness of the magnetic-field amplitudes. The corresponding parts of the phase trajectories are shown in Fig. 3(b) by black solid lines. The peak of the beam can be described by one of the green (dashed) lines in Fig. 3(a) [see also Fig. 3(b)] where the point with $A' = 0$ and $A'' < 0$ (the point of beam maximum) exists. At the beam peak, $A(\xi) > \sqrt{8}$, as it also follows from Eq. (56). Obviously, the transition from tail to peak of the beam is possible only through the jumps between the phase trajectories, as indicated by the dotted arrows in Fig. 3(b). Such jumps are not forbidden if the conditions of continuity of the magnetic $h(\xi)$ and electric $E_x(\xi)$ fields are satisfied. When changing the coordinate ξ , the point (A', A) moves along the route 1-2-3'-2'-1 in Fig. 3(b).

It is convenient to illustrate the beam behavior in the plot $h(A)$, Eq. (56), shown in Fig. 4. The point $(0,0)$ in this plot

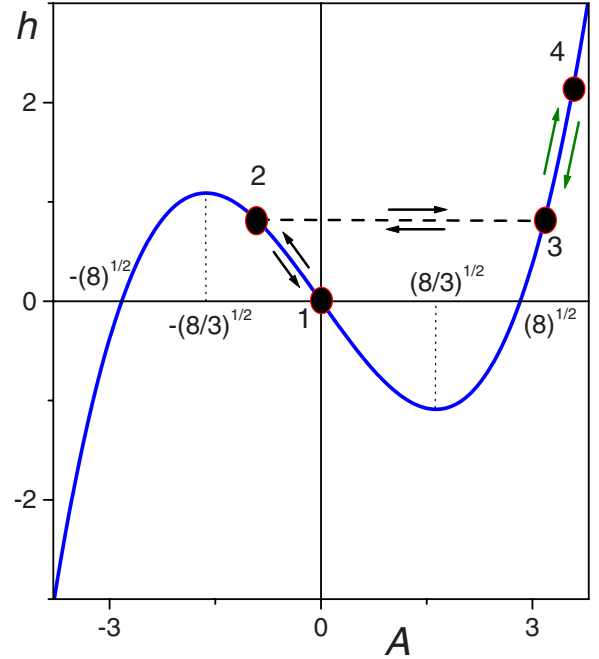


FIG. 4. (Color online) Dimensionless magnetic field $h(A)$ [determined by Eq. (56)] versus amplitude A [defined in Eq. (52)]. The route 1-2-3-4-3-2-1 corresponds to the localized beam profile when the coordinate ξ varies from $-\infty$ to ∞ .

corresponds to $\xi = \pm\infty$. When increasing ξ from $-\infty$, the value of A decreases while h increases (see the route from point 1 to point 2 shown by the arrow in Fig. 4). This movement corresponds to the left tail of the beam. At $A = A_{J1} < 0$, the transition from tail to peak of the beam occurs. This transition is shown in Fig. 4 by the horizontal arrow from point 2 to point 3 with $A = A_{J2} > 2\sqrt{2}$. With further increase of ξ , both values of A and h increase when moving from point 3 to point 4. Point 4 corresponds to the beam maximum, $A(\xi=0) = A_m$ and $h(\xi=0) = h_m$. At $\xi > 0$, we follow the same route, 4-3-2-1, in the reverse direction since the beam is symmetric with respect to $\xi = 0$. The magnetic field is evidently continuous at the points $\xi = \pm\xi_j$ where the jumps occur. The condition of continuity of the electric field E_x determines both the positions $\pm\xi_j$ of the jumps and the values A_{J1} and A_{J2} .

Integrating Eq. (62), we derive the form of the beam for the case $\kappa \gg 1$. For the peak of the beam, the constant G is determined from the condition $A'(0) = 0$, that is, $G = 4(8 - 3A_m^2)^2/3$. So, the peak of the beam is described by the implicit expression,

$$\int_{A_{J2}}^{A_m} \frac{du(3u^2 - 8)}{\sqrt{3(A_m^4 - u^4) - 16(A_m^2 - u^2)}} = 2\kappa|\xi|, \quad |\xi| \leq \xi_j. \quad (63)$$

This equation taken at the point $\xi = \xi_j$,

$$\int_{A_{J2}}^{A_m} \frac{du(3u^2 - 8)}{\sqrt{3(A_m^4 - u^4) - 16(A_m^2 - u^2)}} = 2\kappa\xi_j, \quad (64)$$

relates to the position of the jump with A_{J2} . For the tails of the beam, $G = 256/3$ since $A' = A = 0$ at $|\xi| = \infty$. Thus, we have from Eq. (62)

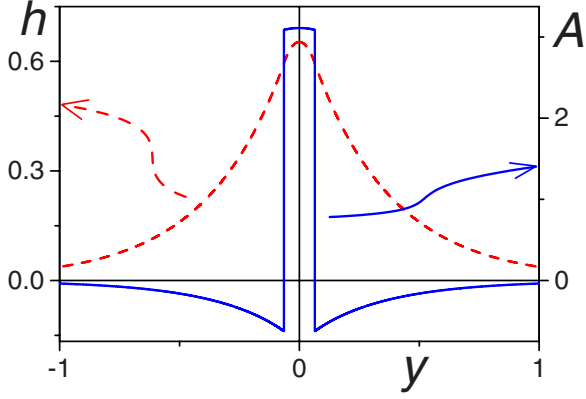


FIG. 5. (Color online) The profile of the localized beam: blue solid line shows the amplitude $A(\xi)$ and the red dashed line shows the dimensionless magnetic field $h(\xi)$. The parameters used here are: $\omega=0.9$, $\kappa=10$, and $A_m=3.5$.

$$\int_{A_{J1}}^{A(\xi)} \frac{du(8-3u^2)}{u\sqrt{16-3u^2}} = 2\kappa(|\xi| - \xi_J), \quad |\xi| > \xi_J. \quad (65)$$

The asymptotics of the $A(\xi)$ dependence when $\xi \rightarrow \infty$, $A \propto \exp(-\kappa\xi)$, coincides with the y -coordinate behavior of the linear surface waves.⁴⁵

The continuity conditions for $h(\xi)$ and $E_x(\xi)$ produce two equations for A_{J1} and A_{J2} :

$$A_{J2} \left(1 - \frac{A_{J2}^2}{8}\right) = A_{J1} \left(1 - \frac{A_{J1}^2}{8}\right),$$

$$A_{J1}^2 - A_{J2}^2 + A_m^2 = \frac{3}{16}(A_{J1}^4 - A_{J2}^4 + A_m^4).$$

Thus, the form of the beam, positions of the jumps, and the values A_{J1} , A_{J2} depend on the parameters ω , κ , and A_m . The form of the beam is illustrated in Fig. 5. The dependences $A(\xi)$ and $h(\xi)$ are shown by the blue solid and the red dashed lines, respectively.

Note that the transverse electric field $E_y(\xi)$ exhibits jumps at the points $\xi = \pm \xi_J$. This means the breaking of charge neutrality at the boundaries between the peak and tails of the beam. However, the results obtained in this section, by solving the simplified Eq. (7), are valid even in this case and there is no need to use the full system of sine-Gordon Eqs. (1) and (2). Indeed, for the parameters used in our calculations, the characteristic sizes of the beam peak and tails are of the order $\xi_J \sim 1$. Correspondingly, the condition

$$\alpha(qD/\lambda_{ab})^2 \ll 1$$

is valid for the obtained solutions and we can neglect the charge neutrality breaking in the beam peak and tails. The analysis of Eqs. (1) and (2) reveals that the spatial scale of the electric-field jump at the peak-tail boundary must be of the order of D . Then, from the mathematical point of view, it is reasonable to treat the peak-tail boundary as the surface of

discontinuity, and match the fields on the left and on the right side at this boundary, which was done in the above considerations.

The obtained results are valid under conditions of sufficiently small dissipation, that is, we have to require that $\nu_c \ll 1 - \omega^2$ and $\nu_{ab} \ll 1$, as it can be seen from Eq. (46) and a simple analysis of our calculations. The next requirement is the smallness of the sample overheating. Using Eqs. (13) and (23), and results shown in Fig. 3, the value of E_y can be estimated as $E_y \sim H_0 \omega \sqrt{8(1-\omega^2)}/\epsilon$ and $E_x \sim qE_y \sqrt{(1-\omega^2)}/\gamma$. Then, similar to Eq. (48), we derive

$$\Delta T \approx \frac{8H_0^2(1-\omega^2)\sigma_c \Delta y}{W\epsilon} \left(1 + \frac{q^2(1-\omega^2)\sigma_{ab}}{\gamma^2\sigma_c}\right), \quad (66)$$

where $2\Delta y = 2\xi_J \lambda_{ab}$ is the thickness of the beam peak, where the main heat release occurs. Assuming that $1 - \omega^2 = 0.01$, we obtain $\Delta T/(T_c - T) \sim 0.5$ K (in liquid helium) and 5×10^{-4} K (in liquid nitrogen) for the parameter values used for the estimates of overheating in Sec. III. Thus, the validity requirement for the existence of a terahertz beam can be satisfied for standard material parameters.

V. CONCLUSIONS

We analyzed theoretically two nonlinear effects for Josephson plasma waves in layered superconductors. One of them is the nonlinear plasma resonance accompanied by the hysteretic behavior of the wave amplitude-frequency dependence. The hysteresis can be observed if the incident wave frequency ω is slightly higher than the Josephson plasma frequency ω_J and the wave amplitude exceeds a threshold value. The hysteretic jumps in the amplitude-frequency dependence give rise to the interesting phenomenon of transforming the continuous input terahertz radiation into a series of short and strong electromagnetic pulses. Another phenomenon considered in this paper is the propagation of a nonlinear terahertz beam localized in the direction across the superconducting layers. This beam can exist at frequencies ω slightly below ω_J . The nontrivial structure of the beam was studied in detail. This phenomenon is an analog of the self-focusing effect in nonlinear optics. These types of nonlinear phenomena in layered superconductors could be used to design a new generation of terahertz devices.

ACKNOWLEDGMENTS

We gratefully acknowledge partial support from the National Security Agency (NSA), Laboratory Physical Science (LPS), Army Research Office (ARO), National Science Foundation (NSF) Grant No. EIA-0130383, JSPS-RFBR No. 06-02-91200, and Core-to-Core (CTC) program supported by Japan Society for Promotion of Science (JSPS). S.S. acknowledges support from the Ministry of Science, Culture and Sport of Japan via the Grant-in Aid for Young Scientists No. 18740224, the EPSRC via No. EP/D072581/1 and No. EP/F005482/1, and ESF network-program ‘‘Arrays of Quantum Dots and Josephson Junctions.’’

- ¹V. L. Pokrovsky, Phys. Rep. **288**, 325 (1997).
- ²T. M. Mishonov, Phys. Rev. B **44**, 12033 (1991).
- ³K. Tamasaku, Y. Nakamura, and S. Uchida, Phys. Rev. Lett. **69**, 1455 (1992).
- ⁴C. C. Homes, T. Timusk, R. Liang, D. A. Bonn, and W. N. Hardy, Phys. Rev. Lett. **71**, 1645 (1993).
- ⁵Y. Matsuda, M. B. Gaifullin, K. Kumagai, K. Kadowaki, and T. Mochiku, Phys. Rev. Lett. **75**, 4512 (1995).
- ⁶Y. Matsuda, M. B. Gaifullin, K. Kumagai, K. Kadowaki, T. Mochiku, and K. Hirata, Phys. Rev. B **55**, R8685 (1997).
- ⁷K. Kadowaki, I. Kakeya, M. B. Gaifullin, T. Mochiku, S. Takahashi, T. Koyama, and M. Tachiki, Phys. Rev. B **56**, 5617 (1997).
- ⁸I. Iguchi, K. Lee, E. Kume, T. Ishibashi, and K. Sato, Phys. Rev. B **61**, 689 (2000).
- ⁹H. B. Wang, P. H. Wu, and T. Yamashita, Phys. Rev. Lett. **87**, 107002 (2001).
- ¹⁰V. K. Thorsmolle, R. D. Averitt, M. P. Maley, L. N. Bulaevskii, C. Helm, and A. J. Teylor, Opt. Lett. **26**, 1292 (2001).
- ¹¹Y. Tominari, T. Kiwa, H. Murakami, M. Tonouchi, H. Wald, P. Seidel, and H. Schneidewind, Appl. Phys. Lett. **80**, 3147 (2002).
- ¹²N. Kameda, M. Tokunaga, T. Tamegai, M. Konczykowski, and S. Okayasu, Phys. Rev. B **69**, 180502(R) (2004).
- ¹³L. Ozyuzer, A. E. Koshelev, C. Kurter, N. Gopalsami, Q. Li, M. Tachiki, K. Kadowaki, T. Yamamoto, H. Minami, H. Yamaguchi, T. Tachiki, K. E. Gray, W.-K. Kwok, and U. Welp, Science **318**, 1291 (2007); L. N. Bulaevskii and A. E. Koshelev, Phys. Rev. Lett. **99**, 057002 (2007); S. Savel'ev, V. Yampol'skii, A. Rakhmanov, and F. Nori, Phys. Rev. B **72**, 144515 (2005); S. Savel'ev, V. Yampol'skii, A. Rakhmanov, and F. Nori, Physica C **437-438**, 281 (2006); **445-448**, 175 (2006).
- ¹⁴S. Savel'ev, A. L. Rakhmanov, and F. Nori, Phys. Rev. Lett. **94**, 157004 (2005); S. Savel'ev, A. L. Rakhmanov, and F. Nori, Phys. Rev. B **74**, 184512 (2006); S. Savel'ev, A. L. Rakhmanov, and F. Nori, Physica C **445-448**, 180 (2006); V. A. Yampol'skii, S. Savel'ev, O. V. Usatenko, S. S. Mel'nik, F. V. Kusmartsev, A. A. Krokhin, and F. Nori, Phys. Rev. B **75**, 014527 (2007).
- ¹⁵S. Savel'ev, A. L. Rakhmanov, and F. Nori, Phys. Rev. Lett. **98**, 077002 (2007); S. Savel'ev, A. L. Rakhmanov, and F. Nori, *ibid.* **98**, 269901(E) (2007); A. O. Sboychakov, S. Savel'ev, A. L. Rakhmanov, and F. Nori, Europhys. Lett. **80**, 17009 (2007); S. Savel'ev, A. O. Sboychakov, A. L. Rakhmanov, and F. Nori, Phys. Rev. B **77**, 014509 (2008).
- ¹⁶J. Zitzmann, A. V. Ustinov, M. Levitchev, and S. Sakai, Phys. Rev. B **66**, 064527 (2002).
- ¹⁷K. Tamasaku, Y. Nakamura, and S. Uchida, Phys. Rev. Lett. **69**, 1455 (1992).
- ¹⁸O. K. C. Tsui, N. P. Ong, Y. Matsuda, Y. F. Yan, and J. B. Peterson, Phys. Rev. Lett. **73**, 724 (1994).
- ¹⁹Y. Matsuda, M. B. Gaifullin, K. Kumagai, K. Kadowaki, and T. Mochiku, Phys. Rev. Lett. **75**, 4512 (1995).
- ²⁰O. K. C. Tsui, N. P. Ong, and J. B. Peterson, Phys. Rev. Lett. **76**, 819 (1996).
- ²¹T. Hanaguri, Y. Tsuchiya, S. Sakamoto, A. Maeda, and D. G. Steel, Phys. Rev. Lett. **78**, 3177 (1997).
- ²²N. F. Pedersen and S. Sakai, Phys. Rev. B **58**, 2820 (1998).
- ²³S. Sakai and N. F. Pedersen, Phys. Rev. B **60**, 9810 (1999).
- ²⁴Ch. Helm and L. N. Bulaevskii, Phys. Rev. B **66**, 094514 (2002).
- ²⁵E. J. Singley, M. Abo-Bakr, D. N. Basov, J. Feikes, P. Guptasarma, K. Hollmack, H. W. Hübers, P. Kuske, M. C. Martin, W. B. Peatman, U. Schade, and G. Wüstefeld, Phys. Rev. B **69**, 092512 (2004).
- ²⁶M. M. Mola, J. T. King, C. P. McRaven, S. Hill, J. S. Qualls, and J. S. Brooks, Phys. Rev. B **62**, 5965 (2000).
- ²⁷M. Tachiki, T. Koyama, and S. Takahashi, Phys. Rev. B **50**, 7065 (1994).
- ²⁸T. Koyama and M. Tachiki, Phys. Rev. B **54**, 16183 (1996).
- ²⁹S. Sakai, P. Bodin, and N. F. Pedersen, J. Appl. Phys. **73**, 2411 (1993).
- ³⁰L. N. Bulaevskii, M. Zamora, D. Baeriswyl, H. Beck, and J. R. Clem, Phys. Rev. B **50**, 12831 (1994).
- ³¹S. N. Artemenko and S. V. Remizov, JETP Lett. **66**, 853 (1997).
- ³²S. N. Artemenko and S. V. Remizov, Physica C **362**, 200 (2001).
- ³³Ch. Helm, J. Keller, Ch. Peris, and A. Sergeev, Physica C **362**, 43 (2001).
- ³⁴Yu. H. Kim and J. Pokharel, Physica C **384**, 425 (2003).
- ³⁵R. Rajaraman, *Solitons and Instantons: An Introduction to Solitons and Instantons in Quantum Field Theory* (North-Holland, Amsterdam, 1982).
- ³⁶O. H. Olsen and M. R. Samuelsen, Phys. Rev. B **34**, 3510 (1986).
- ³⁷Non-technical animations illustrating the nonlinear effects in layered superconductors can be found in <http://dml.riken.jp/nonlinear/nonlinear.swf>
- ³⁸S. Savel'ev, A. L. Rakhmanov, V. Yampol'skii, and F. Nori, Nat. Phys. **2**, 521 (2006).
- ³⁹S. Savel'ev, V. A. Yampol'skii, A. L. Rakhmanov, and F. Nori, Phys. Rev. B **75**, 184503 (2007).
- ⁴⁰A. E. Koshelev and I. Aranson, Phys. Rev. B **64**, 174508 (2001).
- ⁴¹L. N. Bulaevskii and A. E. Koshelev, Phys. Rev. Lett. **99**, 057002 (2007).
- ⁴²S. Rother, Y. Koval, P. Muller, R. Kleiner, D. A. Ryndyk, J. Keller, and C. Helm, Phys. Rev. B **67**, 024510 (2003).
- ⁴³L. D. Landau and E. M. Lifshitz, *Mechanics* (Butterworth-Heinemann, Oxford, 1995).
- ⁴⁴V. S. Vysotsky, Y. A. Ilyin, T. Kiss, M. Inoue, M. Takeo, F. Irie, H. Okamoto, M. Kanazawa, K. Ohya, S. Hayashida, and A. L. Rakhmanov, Cryogenics **40**, 9 (2000); A. L. Rakhmanov, V. S. Vysotsky, Y. A. Ilyin, T. Kiss, and M. Takeo, *ibid.* **40**, 19 (2000).
- ⁴⁵S. Savel'ev, V. Yampol'skii, and F. Nori, Phys. Rev. Lett. **95**, 187002 (2005); Physica C **445-448**, 183 (2006).
- ⁴⁶A. Barone and G. Paterno, *Physics and Applications of the Josephson Effect* (Wiley, New York, 1982).